IAI Journals.ASM.org

Cytokine/Chemokine Secretion and Proteomic Identification of Upregulated Annexin A1 from Peripheral Blood Mononuclear Cells Cocultured with the Liver Fluke *Opisthorchis viverrini*

Nuttanan Hongsrichan,[a,f] Kitti Intuyod,[b,f] Porntip Pinlaor,[c,f] Jarinya Khoontawad,[a,f] Puangrat Yongvanit,[d,f] Chaisiri Wongkham,[d,f] Sittiruk Roytrakul,[e] Somchai Pinlaor[a,f]

Department of Parasitology, Faculty of Medicine, Khon Kaen University, Khon Kaen, Thailand[a]; Biomedical Sciences Program, Graduate School, Khon Kaen University, Khon Kaen, Thailand[b]; Centre for Research and Development in Medical Diagnostic Laboratory, Faculty of Associated Medical Sciences, Khon Kaen University, Khon Kaen, Thailand[c]; Department of Biochemistry, Faculty of Medicine, Khon Kaen University, Khon Kaen, Thailand[d]; Proteomics Research Laboratory, Genome Institute Biotechnology, Pathumthani, Thailand[e]; Liver Fluke and Cholangiocarcinoma Research Center, Faculty of Medicine, Khon Kaen University, Khon Kaen, Thailand[f]

We investigated the cytokine/chemokine secretions and alteration of protein expression from peripheral blood mononuclear cells (PBMCs) cocultured with adult liver flukes (*Opisthorchis viverrini*) for 6 to 24 h. PBMC-derived proteins were identified by two-dimensional electrophoresis and mass spectrometry, and the cytokines/chemokines in the supernatant were assessed using a cytokine array. Exposure to *O. viverrini* induced increases in secretion of proinflammatory cytokines, costimulating protein, adhesion molecules, and chemotactic chemokines relative to untreated controls. In contrast, secretion of the CD40 ligand, interleukin 16, and macrophage inflammatory protein 1β decreased. Proteomic analysis revealed that expression of 48 proteins was significantly altered in PBMCs stimulated with *O. viverrini*. Annexin A1 (ANXA1) was selected for further study, and immunoblotting showed upregulation of ANXA1 expression in PBMCs after 12 and 24 h coculture with liver flukes. In an *in vivo* study, transcription and translation of ANXA1 significantly increased in livers of hamsters infected with *O. viverrini* at 21 days and from 3 months onwards compared to normal controls. Interestingly, immunohistochemistry revealed that ANXA1 was present not only in the cytoplasm of inflammatory cells but also in the cytoplasm of cholangiocytes, which are in close contact with the parasite and its excretory/secretory products in the biliary system. Expression of ANXA1 increased with time concomitant with bile duct enlargement, bile duct formation, and epithelial cell proliferation. In conclusion, several cytokines/chemokines secreted by PBMCs and upregulation of ANXA1 in PBMCs and biliary epithelial cells might have a role in host defense against *O. viverrini* infection and tissue resolution of inflammation.

Opisthorchiasis is caused by infection with the human liver fluke, *Opisthorchis viverrini*, which is endemic in Southeast Asian countries, including Lao People's Democratic Republic, Cambodia, southern Vietnam, and Thailand (1). People can become infected by eating raw, semicooked, or fermented fish, which may be contaminated with metacercariae. Metacercariae excyst in the duodenum and then migrate to and mature in the biliary system. Eggs are produced starting 1 month after infection and are voided with feces. If eggs contaminate a water body, they may be consumed by snails of the genus *Bithynia*, within which cercariae develop. These emerge from the snails and subsequently encyst in cyprinid fish species. Infection with *O. viverrini* is clinically silent in the acute phase but causes hepatobiliary disease during the chronic phase, leading to increased risk of cholangiocarcinoma (CCA) (1, 2). In Thailand, the highest prevalence of opisthorchiasis is found in the northeastern region, where the incidence of CCA is also high (1, 2). At least 10 million people in regions of endemicity are infected with *O. viverrini* and remain at relatively high risk for hepatobiliary disease and CCA (2). Immunopathological processes elicited by the host-parasite interaction are believed to be important mechanisms contributing to opisthorchiasis and CCA (3–5).

Peripheral blood mononuclear cells (PBMCs) consist of lymphocytes and monocytes. These cells are very important immune players and are therefore involved in a large number of diseases. In an opisthorchiasis model, infiltration of mononuclear cells into hamster liver was associated with bile duct epithelium proliferation and periductal fibrosis (6, 7). In contrast, T cell-deprived hamsters showed markedly less inflammatory cell infiltration and liver injury when infected with *O. viverrini* (3). Thus, mononuclear cells might play an important role in pathological changes in opisthorchiasis.

Cytokines and chemokines are secreted by a variety of cell types, including inflammatory cells, and play crucial functions in immunoregulation and immune responses (8), including responses to parasite infection (9, 10). In the hamster opisthorchiasis model, the mRNA expression of Th1 cytokine (interleukin 12 [IL-12]) increased in liver, spleen, and lymph nodes during the acute phase and subsequently switched to Th2 cytokines (transforming growth factor β [TGF-β], IL-4, and IL-10) during the chronic phase (11). In human studies, elevated levels of IL-6 were found in PBMCs stimulated by *O. viverrini* excretory/secretory

Received 22 July 2013 **Returned for modification** 1 September 2013
Accepted 3 March 2014
Published ahead of print 10 March 2014
Editor: J. A. Appleton
Address correspondence to Somchai Pinlaor, psomec@kku.ac.th.
Supplemental material for this article may be found at http://dx.doi.org/10.1128/IAI.00901-13.

doi:10.1128/IAI.00901-13

(ES) products (12) and in plasma (13) of opisthorchiasis patients with advanced periductal fibrosis. Moreover, treatment of a normal immortalized human cholangiocyte cell line with *O. viverrini* ES products also increased the expression of Toll-like receptor 4 (TLR-4) and subsequently stimulated the production of IL-6 and IL-8 (14). In addition, not only cytokines/chemokines but also other molecules, such as the protein peroxiredoxin 6 (Prdx6), a key regulator of the cellular redox balance, might play a role in host defense against *O. viverrini* infection (15). These findings imply that cytokines/chemokines as well as proteins might participate in host responses to *O. viverrini* infection.

However, the identities and expression profiles of the products made by PBMCs in response to *O. viverrini* infection are not well known. We therefore cocultured human PBMCs with adult *O. viverrini* and characterized their cytokine/chemokine secretions using the human cytokine array kit. The PBMC-derived protein expression profile was analyzed using two-dimensional electrophoresis (2DE) followed by liquid chromatography-tandem mass spectrometry (LC/MS-MS). Among the upregulated proteins, annexin A1 (ANXA1) was chosen for further study based on its location in the cell membrane, its increased expression with time after stimulation, and its known involvement in the immune response and carcinogenesis (16). ANXA1 was selected and validated by immunoblotting. In addition, the time profile of ANXA1 expression was investigated in livers of hamsters experimentally infected with *O. viverrini*. This study provides basic information concerning the host-parasite interaction in opisthorchiasis.

MATERIALS AND METHODS

Parasites. *Opisthorchis viverrini* metacercariae were isolated from naturally infected cyprinid fishes obtained from an area of endemicity in Khon Kaen Province, Thailand. Cyprinid fishes were digested by artificial pepsin as previously described (6). In brief, fishes were minced and then homogenized in a blender with 0.25% pepsin–1.5% HCl (Wako Pure Chemical Industries, Osaka, Japan) in 0.85% NaCl solution and incubated for 1 h at 37°C. The digested material was serially filtered (1,000, 300, and 106 μm). Material retained on the 106-μm sieve was washed through a 250-μm sieve using normal saline and then washed several times with normal saline in a sediment jar. Metacercariae were identified and collected from the sediment under a dissecting microscope. Cysts in which movement could be seen were used to infect Syrian golden hamsters by gastric intubation.

Preparation of *O. viverrini* adult worms for *in vitro* coculture. Adult worms were recovered under aseptic conditions from the biliary systems of euthanized hamsters infected 3 to 4 months previously. In order to prevent bacterial contamination, each hamster was sacrificed in a laminar-flow hood using aseptic technique. The live worms were immediately washed several times in phosphate-buffered saline (PBS) with penicillin-streptomycin (100 U/ml) (Gibco Laboratories, Grand Island, NY, USA) to remove any debris and residual blood. Adult worms were then held in RPMI 1640 medium (Invitrogen, Carlsbad, CA, USA) supplemented with penicillin-streptomycin (100 U/ml) and 10% fetal bovine serum (FBS) (Gibco) and incubated at 37°C with 5% CO_2 for 2 h. Only those still actively moving after 2 h were used in the coculture experiment.

Peripheral blood mononuclear cell (PBMC) isolation. Human PBMCs were obtained from the buffy coats of healthy donors at the Blood Bank Center in Srinagarind Hospital, Faculty of Medicine, Khon Kaen University. Five healthy donors that were not infected with hepatitis B or C viruses, human immunodeficiency virus (HIV), *Treponema pallidum*, or *O. viverrini* were enrolled in this study. A dot blot immunoassay was used to confirm that these donors did not have antibodies against *O. viverrini* crude antigen. PBMCs were isolated from the buffy coat using Lymphoprep gradient medium (density, 1.077 g/ml; Axis-Shield PoC AS, Oslo, Norway). PBMCs were subsequently washed with PBS, and the viability of cells was confirmed to be greater than 95% as measured by the trypan blue dye exclusion test. The study protocol was approved by the Ethics Group of the Human Research Committee (protocol no. HE531202), Khon Kaen University, Khon Kaen, Thailand.

PBMCs cocultured with adult *O. viverrini*. Freshly isolated PBMCs from each subject were seeded (1×10^6 cells/well) into wells of a 12-well Transwell culture plate (Costar, Corning Incorporated, Cambridge, NY, USA) in RPMI 1640 medium supplemented with 10% FBS, 1% sodium pyruvate, L-glutamine, and penicillin-streptomycin (100 U/ml). Nine wells were used for each time point to be assayed (three wells for PBMCs cocultured with live flukes, three positive controls, and three negative controls). In each case, PBMCs were grown in the lower chamber of each well for 24 h at 37°C in 5% CO_2 and 95% humidity. For the coculture treatment, *O. viverrini* adult worms (5 worms/well) were then transferred into the upper chamber (separated from the lower by an 8-μm-pore-size plate) and the plates were cultured for 6, 12, and 24 h. Lipopolysaccharide (LPS)-treated PBMCs (1 μg/ml/well) and untreated cells were used as positive and negative controls, respectively. At various time points, cell-free supernatants were collected after centrifugation at 3,000 rpm for 10 min at 4°C and immediately stored at −80°C until cytokine analysis. Cell pellets were washed twice with cold PBS and stored at −80°C until proteomic analysis.

Animal experiments. Use of animals in this study was previously approved by the Animal Ethics Committee of Khon Kaen University, Khon Kaen, Thailand (protocol no. AEKKU17/2550). Fifty male Syrian golden hamsters (*Mesocricetus auratus*) aged 4 to 6 weeks were obtained from the Animal Unit, Faculty of Medicine, Khon Kaen University, Khon Kaen, Thailand. Animals were divided into two groups, the uninfected control group (normal group) and the *O. viverrini*-infected group. Those in the infected group were given 50 metacercariae of *O. viverrini* each. Hamsters were sacrificed at 21 days and 1, 3, 4, and 5 months postinfection ($n = 5$ for each subgroup). For total RNA isolation, liver tissues were immediately transferred to TRIzol reagent (Invitrogen), snap-frozen in liquid nitrogen, and stored at −80°C until use. For Western blotting and 2D Western blotting, liver slices were immediately snap-frozen in liquid nitrogen and stored at −80°C until use. For histopathological study, liver tissues were fixed in 10% buffered formalin, embedded, and sectioned at a 5-μm thickness. Liver tissue sections were stained with hematoxylin and eosin to evaluate histopathological changes.

Two-dimensional electrophoresis. 2DE was performed as previously described (15). PBMCs from each subject and time point were used for 2DE in duplicate experiments. PBMCs were lysed by freeze-thaw and separated into two aliquots, and 500 μl of sample preparation solution (7 M urea, 2 M thiourea, 4% [wt/vol] CHAPS {3-[(3-cholamidopropyl)-dimethylammonio]-1-propanesulfonate}, 2% [vol/vol] immobilized pH gradient [IPG] buffer [pH 3 to 10], 40 mM dithiothreitol [DTT], and protease inhibitors cocktail) (GE Healthcare, Piscataway, NJ, USA) was added to each aliquot. Samples were vortexed, incubated at 4°C for 1 h, and centrifuged at 12,000 rpm for 30 min at 4°C. Protein was precipitated from the supernatant using a 2D cleanup kit (GE Healthcare) and resuspended with sample preparation solution. Protein concentration was measured using the Coomassie plus protein assay (Bio-Rad Laboratories, Hercules, CA, USA) according to the manufacturer's instructions. Thereafter, protein (150 μg) was dissolved in rehydration buffer (7 M urea, 2 M thiourea, 2% [wt/vol] CHAPS, 2% (vol/vol) IPG buffer (pH 3 to 10), 18 mM DTT, and 0.002% bromophenol blue) and loaded onto a 7-cm, pH 3 to 10 nonlinear IPG strip (GE Healthcare). Isoelectric focusing (IEF) was performed using an Ettan IPGphor II isoelectric focusing system at 20°C (GE Healthcare) in a stepwise fashion (30 min, 300 V; 30 min, 1,000-V gradient; 2 h, 5,000-V gradient; 30 min, 5000 V). The strips were equilibrated with 100 mM DTT and 2.5% iodoacetamide according to the instructions of the manufacturer (GE Healthcare). SDS-PAGE was performed using the Mini-Protean Tetra electrophoresis system (Bio-Rad). Briefly, IPG strips were placed on top of 12% polyacrylamide slab gels (8

by 9 by 0.1 cm) and overlaid with 0.5% low-melting-point agarose. The gels were fixed in 45% methanol, 5% acetic acid, and 50% distilled water, followed by staining with 0.25% Coomassie brilliant blue R-250 (USB, Cleveland, OH, USA), and placed overnight in a destaining solution. Gel scanning was performed using ImageScanner (Amersham Biosciences, Cambridge, United Kingdom). Protein spots were analyzed using ImageMaster 2D Platinum software version 6.0 (GE Healthcare). Representative gel images are shown in Fig. S1 in the supplemental material.

Identification of protein spots by mass spectrometry. Protein spots were prepared using tryptic digestion for LC-MS/MS as previously described (17). In brief, the gel spot containing the protein was destained, reduced, and alkylated, and digested with trypsin (Promega, Madison, WI, USA) (10 ng/μl trypsin in 50% acetonitrile–10 mM ammonium bicarbonate). For LC-MS/MS analysis, the proteins were identified using the Water SYNAPT HDMS system (Water Corporation, Milford, MA, USA). The samples were electrosprayed into a mass spectrometer (Synapt HDMS; Waters Corporation). The spectral data were generated in an MS/MS Ion search with Micromass (PKL) file support using the MASCOT engine program (Matrix Science, London, United Kingdom). The MS data were used to query the NCBI database for human proteins. The following search parameters were used in all MS/MS Ion searches: tolerance of one missed cleavage; peptide mass tolerance of ±1.2 Da; fragment mass tolerance of ±0.6 Da; carbamidomethylated cysteine as a fixed modification; oxidation of methionine residues as a variable modification; an electrospray ionization (ESI) ion trap as the instrument type. All identified proteins exhibited a Mascot score of >55, corresponding to a probability of <5% that the observed match is a random event. Moreover, a protein was considered to be correctly identified only when at least 2 peptides matched the same protein with a significant score ($P < 0.05$). For single peptide-based identification, in addition to a significant Mascot score, only peptide sequences with at least three consecutive amino acids detected on MS spectra were considered. These validation criteria were designed to limit the number of false-positive matches without missing real proteins of interest. Molecular function and biological process were assigned to each protein identified according to the UniProt database (Swiss-Prot/TrEMBL) (http://www.uniprot.org) and the Human Protein Reference Database (http://www.hprd.org).

2D-gel Western blotting and Western blot analysis. To verify proteomic data, the expression of ANXA1 in PBMCs was confirmed by 2D-gel Western blotting and Western blot analysis. For 2D-gel Western blotting, PBMC protein (150 μg) from each subject and time point was subjected to 2D gel electrophoresis and transferred to a polyvinylidene difluoride (PVDF) membrane (Amersham Bioscience) using a mini-Trans-Blot system (Bio-Rad) for 2 h at 60 V. For Western blotting, 20 μg of proteins from PBMCs was separated on a 12% SDS-PAGE gel and transferred to a PVDF membrane. The membranes were blocked with 5% skim milk powder in phosphate-buffered saline (PBS) with 0.1% Tween 20 (PBS-T, pH 7.5) for 1 h at room temperature. Then the membranes were incubated with rabbit polyclonal anti-annexin A1 in 2% skim milk–PBS-T (1:1,000; Santa Cruz Biotechnology, Santa Cruz, CA) at 4°C overnight. After washing with 0.1% PBS-T, the membranes were incubated with a 1:3,000 dilution of horseradish peroxidase (HRP)-conjugated secondary antibody (GE Healthcare) diluted in 2% skim milk–PBS-T for 1 h at room temperature. Immunodetection was accomplished with an enhanced chemiluminescence (ECL) Western blotting detection reagent (Amersham Bioscience). Relative band intensity was determined using ImageQuant TL software v2005 (1.1.0.1) (Nonlinear Dynamics, Durham, NC). In addition, hamster liver (approximately 150 mg) was homogenized and protein was extracted as previously described (15). The expression of ANXA1 was also verified in each hamster liver infected with *O. viverrini* by Western blotting using the same protocol as above.

Immunohistochemistry. To investigate ANXA1 expression in *O. viverrini*-infected hamsters, sections cut from each liver were deparaffinized in xylene and then rehydrated through a series of ethanol concentrations. Antigen retrieval was performed by incubating the tissue in 0.01 M citric acid buffer (pH 6.0) and autoclaving at 110°C for 10 min. Endogenous peroxidase activity was eliminated by incubation for 20 min in 3% hydrogen peroxide in PBS. After being washed in PBS, specimens were blocked with 5% FBS for 30 min at room temperature and then incubated with 1:100 rabbit polyclonal anti-annexin A1 (Santa Cruz Biotechnology) at 4°C overnight. Next, the sections were incubated with HRP-conjugated goat anti-rabbit IgG antibody (1:400; GE Healthcare) for 1 h at room temperature and detected using 3,3′-diaminobenzidine tetrahydrochloride (DAB). Sections were counterstained with hematoxylin for 1 min.

The immunohistochemical staining density and intensity in hamster tissue was scored. In brief, the intensity of protein expression was graded as follows: 0, no staining; 1+, mild; 2+, moderate; 3+, strong. The staining density was quantified as the percentage of cells stained positively in tissue as follows: 0, no staining; 1, positive staining in <25%; 2, positive staining in 25 to 50%; 3, positive staining in >50%. The intensity score was multiplied by the density score to yield an overall score of 0 to 9 for each specimen.

Quantitative real-time reverse transcriptase PCR. Real-time RT-PCR was performed in the Applied Biosystems 7500 thermal cycler (Applied Biosystems, Foster City, CA, USA). Total RNA was isolated from hamster livers, and cDNA synthesis was performed using Superscript II reverse transcriptase (Invitrogen) according to the manufacturer's protocol. Real-time RT-PCR was performed in duplicate experiments on each hamster liver using the primers ANXA1-F (5′-GCTCAGTTTGATGCAG ATGAAC-3′) and ANXA1-R (5′-GATGTCTTTGGCCAGATCTC-3′) and the FastStart universal SYBR green master (Rox) kit (Roche Applied Science, Mannheim, Germany) as described previously (6). This pair of primers was designed to amplify a 159-bp fragment from the rat *ANXA1* gene. The operation was performed as following conditions: 95°C for 10 min, followed by 35 cycles of denaturation at 95°C for 15 s, annealing at 55°C for 30 s, and extension at 72°C for 1 min. All data were analyzed using Rotor Gene 5 software (Corbett Research, Sydney, NSW, Australia) with a cycle threshold (C_T) in the linear range of amplification. Relative quantification of *ANXA1* mRNA expression was determined using glyceraldehyde-3-phosphate dehydrogenase (GAPDH) as an internal control using the $2^{-\Delta\Delta CT}$ method.

Cytokine arrays. Human cytokines in pooled cell culture supernatants from each time point were measured using the Proteome Profiler human cytokine panel A array kit (R&D Systems, Minneapolis, MN, USA) according to the manufacturer's instructions. The kit consists of a nitrocellulose membrane containing 36 different anti-cytokine/chemokine antibodies spotted in duplicate. The 36 cytokines/chemokines included complement component 5a (C5a), CD40 ligand, granulocyte colony-stimulating factor (G-CSF), granulocyte-macrophage colony-stimulating factor (GM-CSF), GROα, I-309, soluble intercellular adhesion molecule 1 (sICAM-1), gamma interferon (IFN-γ), IL-1α, IL-1β, IL-1ra, IL-2, IL-4, IL-5, IL-6, IL-8, IL-10, IL-12p70, IL-13, IL-16, IL-17, IL-17E, IL-23, IL-27, IL-32α, IFN-γ-induced protein 10 (IP-10), I-TAC, monocyte chemoattractant protein 1 (MCP-1), migration inhibition factor (MIF), macrophage inflammatory protein 1α (MIP-1α), MIP-1β, serpin E1, RANTES, SDF-1, tumor necrosis factor alpha (TNF-α), and sTREM-1. Briefly, membranes were incubated with blocking buffer at room temperature for 1 h. Cell supernatants (0.5 ml) were mixed with a biotinylated detection antibody cocktail at room temperature for 1 h, and then each was incubated with a membrane overnight at 4°C. The arrays were then washed three times for 10 min and subsequently incubated with horseradish peroxidase-conjugated streptavidin for 30 min at room temperature. The arrays were exposed to peroxidase substrate (ECL Western blotting detection reagent; Amersham Bioscience). Array images were exposed to X-ray film and scanned for pixel density analysis using ImageQuant TL software (GE Healthcare). The data were expressed as the change in expression of cytokines/chemo-

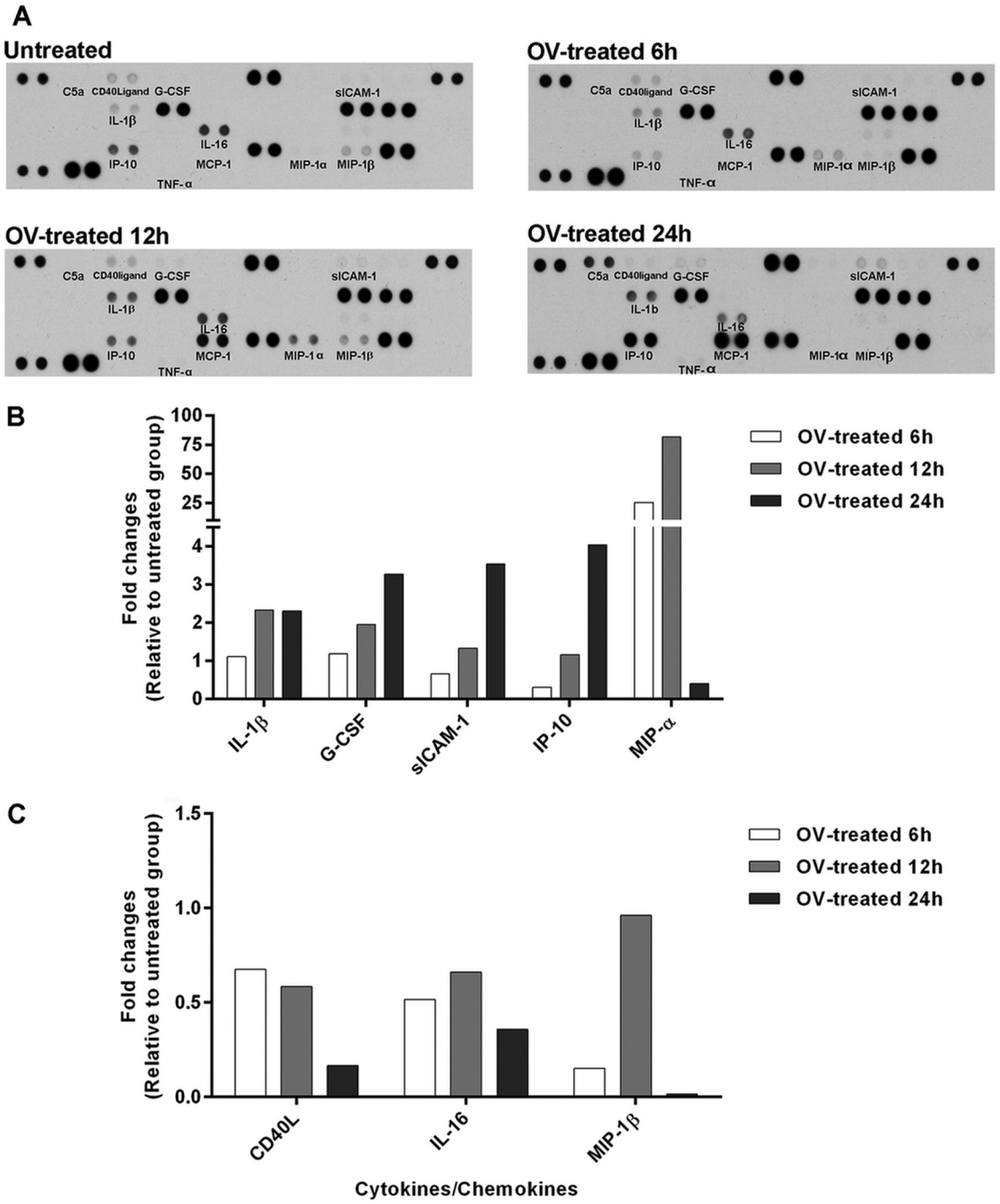

FIG 1 Array analysis of cytokine and chemokine secretion by PBMCs (10^6 cells/ml) cocultured with *O. viverrini* (OV) in Transwell plates for 6, 12, or 24 h. Pooled culture medium obtained from each time point was assayed for production of cytokines/chemokines. Array images show spots of each cytokine or chemokine detected from untreated and OV-treated PBMCs at 6, 12, and 24 h (A). The ratio of mean pixel densities in OV-treated PBMCs to that in controls is presented as fold increase (B) or decrease (C).

kines of treated PBMCs relative to that of the corresponding cytokines/chemokines of untreated PBMCs.

Statistical analysis. The data are presented as means ± standard deviations (SD). To compare the expression levels of protein between treated and untreated PBMC groups, statistical significance of spot intensity of proteomic data was determined using Student's *t* test. Relative gene expression levels were assessed by one-way analysis of variance (ANOVA). A nonparametric Mann-Whitney *U* test was used to compare the immunohistochemistry expression level of ANXA1 in hamster data. Statistical analysis was performed using SPSS version 15 (SPSS Inc., Chicago, IL, USA). A P value of <0.05 was considered statistically significant.

RESULTS

Cytokine/chemokine secretion from PBMCs induced by *O. viverrini*. Pooled supernatants obtained from human PBMCs

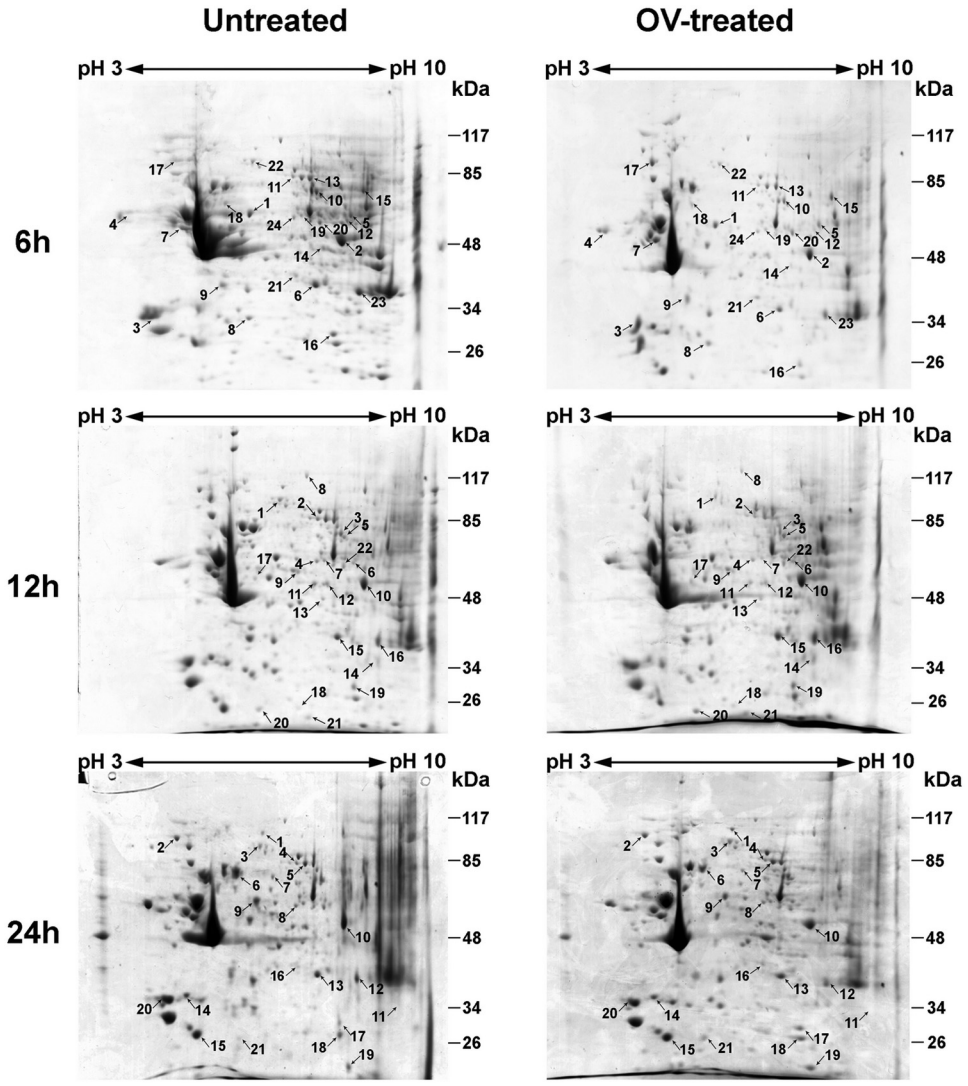

FIG 2 2D electrophoresis of human PBMCs treated with *O. viverrini* (OV) for 6, 12, and 24 h and untreated PBMCs. IEF was performed with total protein extracted from PBMCs in the pH range from 3 to 10 (nonlinear), separated on 12% polyacrylamide gels, and stained with Coomassie brilliant blue R-250. Spots showing differential expression and the corresponding proteins were identified using LC-MS/MS and database searching. The spot numbers on the gels correspond to the numbers in Table 1.

cocultured with *O. viverrini* for 6, 12, and 24 h at 37°C were used for cytokine array analysis. The array images are shown in Fig. 1A. Secretion of proinflammatory cytokines (IL-1β), costimulating protein (G-CSF), adhesion molecule (sICAM-1), and chemotactic chemokines (IP-10 and MIP-1α) increased in supernatants of PBMCs incubated with *O. viverrini*. Expression of proinflammatory cytokines (TNF-α) and chemotactic chemokines (C5a and MCP-1) occurred in supernatants from treated PBMCs but not in untreated controls. Secretion levels of sICAM-1, G-CSF, IL-1β, and IP-10 increased with time of stimulation, while levels of MIP-1α peaked at 12 h and subsequently decreased (Fig. 1B). In contrast, levels of CD40 ligand (CD40L), IL-16, and MIP-1β were reduced by *O. viverrini* stimulation (Fig. 1C). Secretion of GM-CSF, GROα, I-309, IFN-γ, IL-1α, IL-1ra, IL-2, IL-4, IL-5, IL-6, IL-8, IL-10, IL-12p70, IL-13, IL-17, IL-17E, IL-23, IL-27, IL-32α, I-TAC, MIF, serpin E1, RANTES, SDF-1, and sTREM-1 could not be detected in any array, control, or experiment.

Proteomic identification of proteins in human PBMCs stimulated with *O. viverrini*. 2DE and LC-MS/MS-based proteomic approaches were used to analyze protein expression in PBMCs after cocultivation with *O. viverrini* for 6 to 24 h. Forty-eight proteins were significantly up- or downregulated in treated PBMCs relative to untreated PBMCs, as shown in Fig. 2 and Table 1. The identified proteins were classified according to their known or predicted cellular localizations and biological functions according to the UniProt knowledgebase (Swiss-Prot/TrEMBL) and the Human Protein Reference database (Fig. 3). Proteins were typically located in the cytoplasm (59%), nucleus (17%), mitochondrion (8%), endoplasmic reticulum (8%), plasma membrane (6%), and ribosome (2%) (Fig. 3A). Of these proteins, 29% were associated with metabolism, 17% were associated with signal transduction, 15% were structural, 13% were associated with the immune response, 8% were associated with transport, 6% were associated with translation, 4% were associated with the cell cycle and with

TABLE 1 Proteins identified by LC-MS/MS according to biological process, localization, and pattern of expression profile

Category and spot no.[a]	Protein name	Accession no.	Localization	Score[b]	Coverage[c] (%)	No. of peptides matched[d]	pI	Nominal mass	Change in expression at[e]: 6 h	12 h	24 h
Immune response											
6 h, no. 6	Annexin A1	NP_000691	Plasma membrane	516	33	11	6.57	38,918	Down	Up	Up
12 h, no. 15				651	38	11	6.57	38,918			
24 h, no. 13				557	39	13	6.57	38,918			
24 h, no. 7	Leukotriene A4 Hydrolase	1GW6_A	Cytoplasm	340	18	9	5.87	69,736	—	—	Down
6 h, no. 13	Moesin	EAX05399	Cytoplasm	360	20	12	5.9	66,678	Down	—	Down
24 h, no. 5				202	11	9	6.08	67,892			
12 h, no. 21	Protein DJ-1	NP_009193	Cytoplasm	79	25	5	6.33	20,050	—	Down	—
24 h, no. 9	Tapasin	3F8U_A	Endoplasmic reticulum	454	23	11	5.61	54,541	—	—	Down
6 h, no. 5	T-cell receptor β chain	AAC96236	Plasma membrane	55	34	4	12.22	4,975	Up	—	—
Metabolism											
24 h, no. 1	Alpha glucosidase II α subunit	AAH65266	Endoplasmic reticulum	69	3	5	5.36	96,475	—	—	Down
12 h, no. 13	Aryl hydrocarbon receptor nuclear translocator	CAB65056	Nucleus	62	89	5	9.97	2,403	—	Down	—
6 h, no. 7	ATP synthase β	ABD77240	Mitochondrion	849	45	25	4.95	48,083	Down	—	—
6 h, no. 4	Calreticulin	BAD96780	Endoplasmic reticulum	103	9	6	4.3	47,061	Up	—	—
6 h, no. 18	CCT8 protein	AAH12584	Cytoplasm	115	11	7	5.18	54,585	Down	—	—
6 h, no. 14	Elongation factor Tu	AAB00499	Mitochondrion	308	17	7	7.7	49,851	Down	—	—
6 h, no. 2	Enolase 1	NP_001419	Cytoplasm	504	27	13	7.01	47,481	Down	Up	Up
12 h, no. 10				734	35	17	7.01	47,481			
24 h, no. 10				487	23	9	7.01	47,481			
12 h, no. 20	Glutathione Transferase P1-1	1EOH_A	Cytoplasm	441	48	12	5.74	23,394	—	Up	—
12 h, no. 23	L-Lactate dehydrogenase	NP_002291	Cytoplasm	339	21	11	5.71	36,900	—	Down	—
6 h, no. 16	Phosphoglycerate mutase 1	AAH62302	Cytoplasm	290	41	8	6.67	28,916	Down	Up	Up
12 h, no. 19				120	21	3	6.67	28,916			
24 h, no. 17				109	21	3	6.67	28,916			
6 h, no. 8	Proteasome activator complex subunit 1	NP_006254	Cytoplasm	378	42	13	5.78	28,876	Up	—	—
24 h, no. 19	Superoxide dismutase 2	AAP34408	Mitochondrion	227	22	5	6.87	23,324	—	—	Up
6 h, no. 24	T-complex protein 1 subunit β isoform 1	NP_006422	Cytoplasm	334	19	13	6.01	57,794	Down	Down	Down
12 h, no. 4				351	17	9	6.10	61,066			
24 h, no. 8				317	17	11	6.03	60,869			
24 h, no. 18	Triosephosphate isomerase 1	NP_000356	Cytoplasm	405	48	13	6.45	26,938	—	—	Up
Signal transduction											
6 h, no. 23	Annexin A2	NP_004030	Nucleus	484	31	9	7.57	38,808	Down	Up	Up
12 h, no. 16				518	24	9	7.57	38,808			
24 h, no. 12				578	28	9	7.57	38,808			
12 h, no. 18	Annexin A4	BAD92694	Nucleus	248	21	7	6.03	25,633	—	Down	—
24 h, no. 14	Annexin A5	NP_001145	Cytoplasm	408	28	13	4.94	35,971	—	—	Up
6 h, no. 12	CAP[f]	EAX07240	Cytoplasm	126	8	4	7.64	51,357	Down	—	—
6 h, no. 15	Discoidin domain receptor 2	AAH02433	Plasma membrane	282	24	10	8.02	50,335	Up	—	—
12 h, no. 5	Hsp70/Hsp90 protein	XP_001691869	Nucleus	207	11	10	7.81	68,721	—	Up	—
12 h, no. 14	Lim and SH3 protein 1	AAH12460	Cytoplasm	111	17	10	8.06	30,038	—	Down	—
12 h, no. 9	Rho GTPase-activating protein 1	NP_004299	Cytoplasm	412	31	3	6.11	51,087	—	Down	—
Stress response											
6 h, no. 17	Heat shock protein 90	AAI08696	Cytoplasm	474	24	21	5.11	68,614	Up	—	—
24 h, no. 2	Tumor rejection antigen 1	NP_003290	Endoplasmic reticulum	571	16	15	4.76	92,696	—	—	Down
Structure											
6 h, no. 1	Actin-related protein 3	NP_005712	Cytoplasm	308	19	12	5.61	47,797	Down	—	—
6 h, no. 11	Ezrin	NP_003370	Cytoplasm	456	16	13	5.94	69,484	Down	Down	Down
12 h, no. 2				493	20	15	5.94	69,484			
24 h, no. 4				421	15	11	5.94	69,484			
6 h, no. 9	F-actin-capping β subunit	NP_004921	Cytoplasm	286	26	7	5.69	30,952	Up	—	—
6 h, no. 22	Gelsolin	NP_937895	Cytoplasm	74	9	3	5.58	80,876	Down	Down	Down
12 h, no. 1				165	7	11	5.58	80,876			
24 h, no. 3				208	9	11	5.58	80,876			

6 h, no. 3	Tropomyosin 3	NP_705935	Cytoplasm	221	18	7	4.70	28,800	Up	—	Down
24 h, no. 20				129	18	7	4.75	29,243			
12 h, no. 8	Vinculin	NP_003364	Cytoplasm	441	13	16	5.83	117,220	—	Down	—
6 h, no. 10	WDR1 protein	AAD05045	Cytoplasm	268	16	6	6.41	58,593	Down	Down	—
12 h, no. 3				297	19	10	6.41	58,593			
Cell cycle											
12 h, no. 6	Annexin A11	NP_001148	Cytoplasm	387	16	8	7.53	54,697	—	Down	—
6 h, no. 20	Septin 6	NP_665798	Nucleus	337	26	15	6.35	49,184	Down	Down	—
12 h, no. 22				129	7	5	6.35	49,184			
Transcription											
6 h, no. 21	LIM domain binding	AAC05580	Cytoplasm	265	18	7	6.8	36,604	Up	—	Up
24 h, no. 16				210	15	7	6.8	36,604			
Translation											
12 h, no. 12	DEAD box protein 48	NP_055555	Nucleus	268	29	12	6.3	47,126	—	Down	—
6 h, no. 19	Pre-mRNA-processing factor 19	NP_055317	Nucleus	115	9	6	6.14	55,603	Down	Down	—
12 h, no. 7				141	14	6	6.14	55,603			
24 h, no. 11	Ribosomal protein L4	EAW77773	Ribosome	77	15	8	11.03	37,861	—	—	Down
Transport											
24 h, no. 6	Annexin A6	NP_001180473	Cytoplasm	606	33	23	5.42	72,720	—	—	Down
24 h, no. 15	Chloride intracellular channel 1	NP_001279	Nucleus	337	26	9	5.02	27,249	—	—	Down
24 h, no. 21	Ferritin heavy chain 1	EAW73993	Cytoplasm	70	15	4	6.04	26,374	—	—	Up
12 h, no. 11	GDP dissociation inhibitor 2	NP_001485	Cytoplasm	412	31	15	6.11	51,087	—	Down	—
Unknown											
12 h, no. 17	Glyoxalase domain-containing protein 4	NP_057164	Mitochondrion	142	12	4	5.4	33,554	—	Down	—

[a] The spot numbers correspond to the numbers on the 2D gels in Fig. 2.

[b] Probability score in Mascot program (a Mascot score of >55 corresponds to a probability of <5% that the observed match is a random event).

[c] Percent coverage of the matched peptide in relation to the full-length sequence.

[d] Number of matched peptides in database search.

[e] Down, significantly downregulated ($P < 0.05$); up, significantly upregulated ($P < 0.05$); —, no significantly change in expression compared with control.

[f] Adenylate cyclase-associated protein.

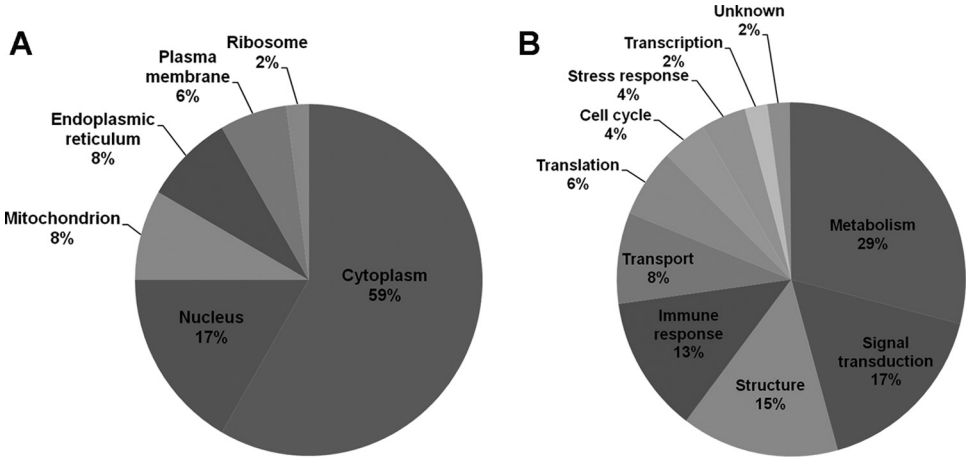

FIG 3 Cellular localization and functional categories of the 48 differentially expressed proteins in human PBMCs stimulated with *O. viverrini*. The identified proteins were classified according to their known or predicted cellular localizations and biological functions according to the Human Protein Reference Database and the UniProt database. The pie chart shows the proportion of identified proteins based on cellular localization (A) and functional category (B).

stress response, 2% were associated with transcription, and 2% were unknown (Fig. 3B).

Validation of annexin A1 in *O. viverrini*-stimulated PBMCs. Following the above bioinformatics analysis, ANXA1 protein was selected for further study due to (i) its increased expression with time (upregulated 1.44-fold and 3.50-fold at 12 and 24 h, respectively), (ii) its location at the cell membrane, (iii) its involvement in immune response and signal transduction, and (iv) the fact that its expression has never been reported in opisthorchiasis. Western blotting showed that expression of ANXA1 significantly increased in PBMCs after 12 and 24 h of coculture with *O. viverrini* (Fig. 4A). In addition, expression of ANXA1 was unchanged in untreated controls at every time point. Moreover, 2D Western blotting also revealed that upregulated expression of ANXA1 (pI $\approx$ 6.5, molecular mass = 38 kDa) was 3.7-fold higher in *O. viverrini*-treated PBMCs than untreated controls at 24 h (Fig. 4B, C, and D).

Expression of annexin A1 in *O. viverrini*-infected hamsters. In liver sections, faint immunoreactivity of ANXA1 was found in biliary epithelial cells of normal liver (Fig. 5A) and was unchanged with a similar scoring at any time point (1 ± 0.00 at 1, 3, and 5 months). In *O. viverrini*-infected hamsters, ANXA1 was observed not only in inflammatory cells but also in bile duct epithelial cells (Fig. 5B to F). Expression of ANXA1 was found in the cytoplasm of inflammatory cells, mainly in some large cells (macrophage-like cells) at aggregations of lymphoid cells surrounding the parasite in the bile duct lumen (Fig. 5E). Interestingly, expression of ANXA1 in cholangiocytes was found not only in the lumen of large bile ducts, where worms reside, but also in small bile ducts and ductules lacking parasites (Fig. 5F). Early in the course of infection, ANXA1 was expressed mainly in inflammatory cells and peaked at 3 months (Fig. 5C). At 5 months, ANXA1 expression in inflammatory cells tended to be lower (Fig. 5D), whereas its expression in bile duct epithelial cells increased with time as bile ducts enlarged and small bile ducts proliferated. The score of ANXA1 expression at 5 months was significantly higher than at 3 months (7 ± 1.73 versus 4 ± 0.00; $P < 0.05$) and at 3 months was much higher than at 1 month (4 ± 0.00 versus 2 ± 0.00; $P < 0.05$).

To compare levels of translation and transcription of ANXA1 in hamster liver over time, Western blotting and real-time RT-PCR were used. Western blot analysis showed that expression level of ANXA1 protein in liver homogenate significantly increased earlier, at 21 days, and then increased from 3 months onwards compared to normal controls (Fig. 6A). In addition, the relative mRNA expression levels of ANXA1 significantly increased at 21 days and 3, 4, and 5 months postinfection (Fig. 6B).

DISCUSSION

To obtain a more comprehensive picture of the global impact on the response by PBMCs against *O. viverrini*, we cocultivated healthy human PBMCs with live worms and investigated protein expression using a proteomic approach and cytokine/chemokine secretion using a cytokine array assay. We have clearly demonstrated that stimulation of PBMCs with products from live flukes leads to the secretion of many cytokines/chemokines from PBMCs and changes in protein expression. Several cytokines and chemokines were upregulated, including proinflammatory cytokines (IL-1β, TNF-α, and G-CSF), a cell adhesion molecule (sICAM-1), and chemoattractant chemokines (MCP-1, MIP-1α, IP-10, and C5a). TNF-α is a cytokine that plays a critical role in the regulation of inflammatory processes, both idiopathic and against infectious agents (18). In parasite infection, TNF-α can induce nitric oxide production by activated macrophages, which leads to parasite death (19, 20). IL-1β is a proinflammatory cytokine which participates in inflammatory responses by induction of inducible nitric oxide synthase (iNOS) and COX-2 expression (21). Previously, we demonstrated upregulation of iNOS and COX-2 in macrophages treated with *O. viverrini* crude antigen (22) and in the livers of hamsters infected with *O. viverrini*. This upregulation can be detected in hamsters from as little as 3 days postinfection and persists until the late phase of infection (23). Expression of iNOS leads to the production of nitric oxide, which is important for host defense against some bacterial, protozoal, and helminthic infections (24–26). Furthermore, IL-1β and TNF-α can induce the expression of sICAM-1, a circulating form of ICAM-1 (27), which participates in leukocyte adhesion and facilitates leukocyte transendothelial migration (28). Thus, production of IL-1β and

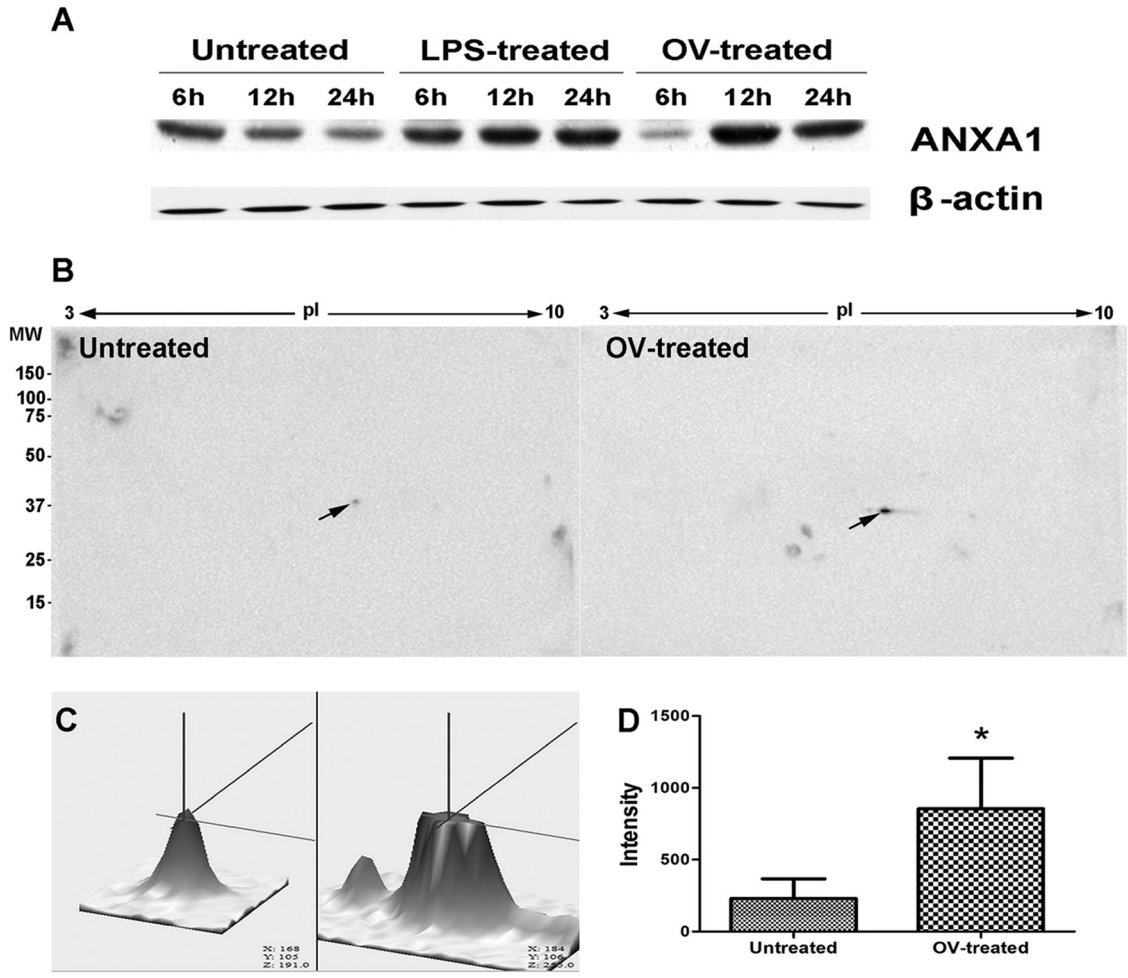

FIG 4 Validation of ANXA1 expression in human PBMCs stimulated with *O. viverrini* (OV) by immunoblotting analysis. Western blot analysis shows upregulation of ANXA1 at 12 and 24 h (A), as does 2DE-Western blotting after 24 h (B: arrow points to spot of ANXA1). 3D images (C) show a 3.7-fold increase of intensity of ANXA1 expression in the treated group relative to the control group (D). Statistical comparison with untreated control (D). *, $P < 0.05$.

TNF-α by *O. viverrini*-stimulated PBMCs may be a component of host defense against the parasite.

Chemoattractant chemokines, including MIP-1α, MCP-1, IP-10, and C5a, were also elevated in *O. viverrini*-stimulated PBMCs. These chemokines are involved in the cellular recruitment and activation of several leukocytes such as monocytes/macrophages, polymorphonuclear cells, and lymphocyte infiltration to the sites of infection (29–32). In the initial phase of *O. viverrini* infection (days 3, 7, and 15), the inflammatory cells infiltrating the portal areas consist of a large number of eosinophils with some neutrophils and mononuclear cells and contribute to the development of microgranulomas. Thereafter, there was an increase in mononuclear cells and a decline of eosinophils (7). However, *O. viverrini* infection in T cell-deprived hamsters showed a marked decrease in the intensity of the periportal inflammation compared with intact hamsters (3). Thus, the chemokine response in *O. viverrini*-stimulated PBMCs may participate in the host defense mechanism as well as in pathogenesis of opisthorchiasis.

In contrast, secretion of CD40 ligand (CD40L), interleukin-16 (IL-16), and macrophage inflammatory protein 1β (MIP-1β) decreased in PBMCs stimulated with *O. viverrini*. CD40-CD40L interactions have been shown to be essential for immunity to some parasite infection (33). The reduction of CD40L caused by *O. viverrini* infection may be associated with parasite survival. In addition, several Th2 (IL-4, IL-5, IL-10, and IL-13), and Treg (IL-17, IL-17E, and IL-23) cytokines were undetectable in PBMCs stimulated with *O. viverrini* in this experiment, suggesting that these cytokines/chemokines are involved in the chronic-phase response. This assumption was supported by the evidence that expression of Th2 cytokines (TGF-β, IL-4, and IL-10) could be detected in chronically *O. viverrini*-infected hamsters (11).

Previously, we established that *O. viverrini* crude antigen extract induces leukocytes (34) and mouse macrophage cell lines (22) to engage in host-parasite interactions. Here, we used a proteomic approach to discover all possible protein responses to liver fluke infection. A total of 48 PBMC proteins, located in various cellular compartments, were upregulated and/or downregulated compared with unstimulated PBMCs. These proteins were functionally associated with metabolism, signal transduction, cell structure, immune response, etc., demonstrating the very broad response by PBMCs after stimulation with *O. viverrini*.

Because membrane proteins are known to play a crucial role in host-parasite interaction, we selected ANXA1 for further valida-

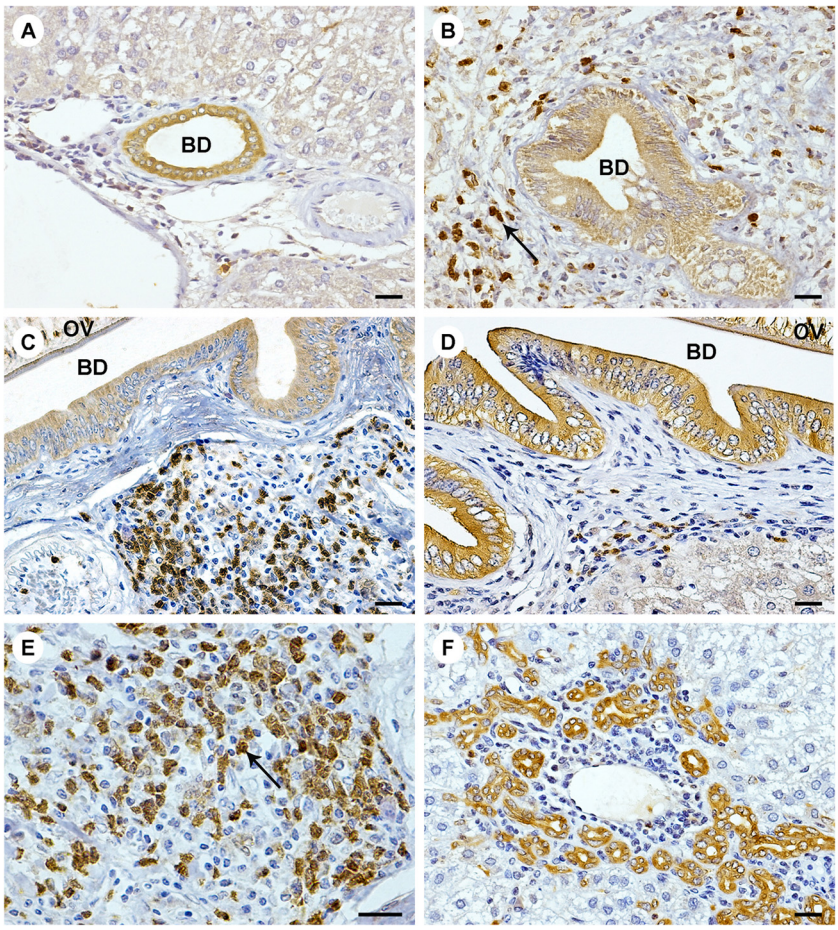

FIG 5 Immunohistochemistry of ANXA1 expression in livers of hamsters infected with *O. viverrini*. Immunohistochemistry was performed in normal hamster liver at 5 months (A) and in *O. viverrini*-infected livers at 1 month (B), 3 months (C), and 5 months (D). A single representative image is shown for each time point (5 liver samples per time point). ANXA1 was expressed in the cytoplasm of inflammatory cells (arrow [B and E]) and proliferating bile duct epithelial cells (F). The magnification is ×400, except in panel E, where it is ×600 (scale bar = 200 μm). BD, bile duct; OV, *Opisthorchis viverrini*.

tion based on its locality in the cell, its pattern of expression, and its functional activity. ANXA1 belongs to the annexin superfamily of proteins and binds to cellular membranes in a Ca^{2+}-dependent manner (35). It is localized in the cytoplasm and is translocated to the cellular membrane after posttranslational modification (36). ANXA1 is involved in a broad range of molecular and cellular processes, including anti-inflammatory signaling, kinase activities in signal transduction, maintenance of cytoskeleton and extracellular matrix integrity, tissue growth, apoptosis, and differentiation (37). Increase of ANXA1 expression in inflammatory cells has been detected in mice infected with *Toxoplasma gondii* (38). We hypothesize that ANXA1 might play a role in host-parasite interactions in *O. viverrini* infection.

The initial stages of inflammation are modulated by multiple interactions involving cell adhesion molecules, cytokines, and chemokines to recruit leukocytes to the site of infection. In animal models of arthritis, ANXA1 is expressed in leukocytes, has anti-inflammatory effects through proinflammatory stimuli such as IL-1β, and participates in the regulatory control of inflammation (39). Relevantly, an increased level of IL-1β may mediate ANXA1 expression in *O. viverrini*-stimulated human PBMC. Consequently, ANXA1 might play a role in host defense and phagocytosis via its receptor, formyl peptide receptor type 2 (40). Moreover, in livers of hamsters infected with *O. viverrini*, expression of ANXA1 increased early (at 21 days), suggesting that it is responding to proinflammatory cytokines such as IL-1β.

Expression of ANXA1 was found not only in inflammatory cells but also in biliary epithelial cells and increased in a time-dependent manner as bile ducts enlarged and their epithelium proliferated. An increase of ANXA1 in bile duct epithelial cells with time may be a response to excretory/secretory products of parasites as worms mature. Its expression may also mediate the resolution of inflammation (35) during long-term infection by involving the progression of fibrosis (41). Thickening of periductal fibrosis, a characteristic of chronic opisthorchiasis (2, 6, 7), is accompanied by the proliferation of bile duct epithelium, in which ANXA1 was strongly expressed (Fig. 5F). This increased expression might be related to healing of damage to bile ducts and liver tissue (42) caused by *O. viverrini* infection, comparable to the ability of ANXA1 to restore skeletal muscle tissue (37). In contrast, expression of ANXA1 in inflammatory cells increased at 3 months and then decreased by 5 months, perhaps as a consequence of immunosuppression during the chronic phase of opisthorchiasis (7, 43, 44). ANXA1 is an anti-inflammatory mediator capable of

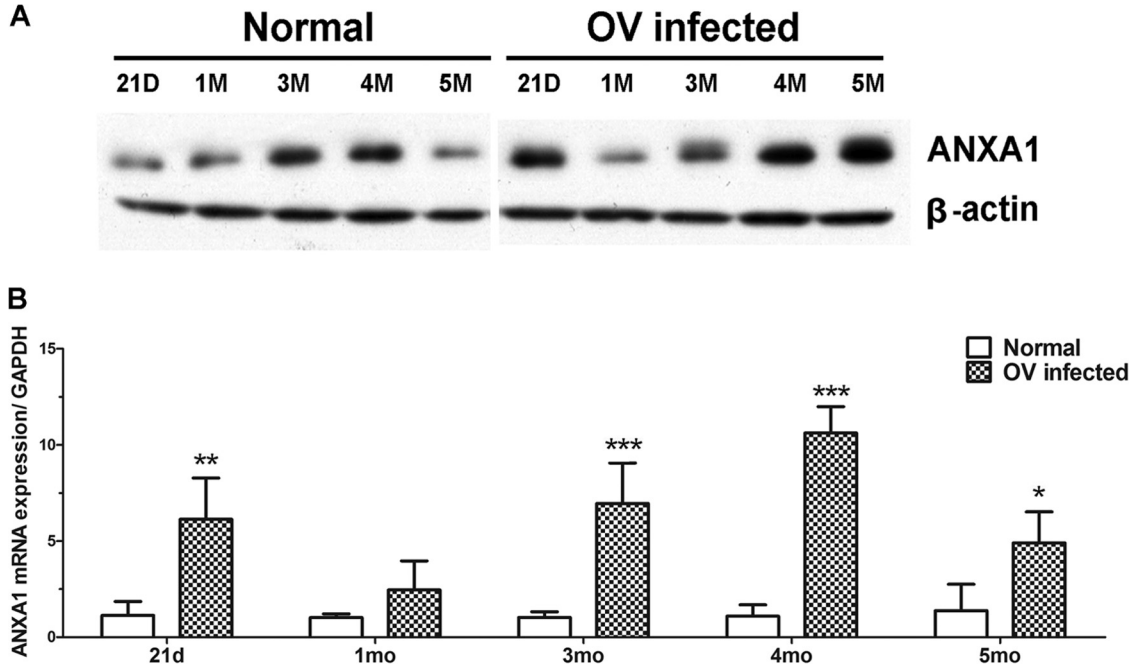

FIG 6 Time profile expression of ANXA1 in *O. viverrini*-infected hamsters. (A) Western blot analysis of ANXA1 in livers of *O. viverrini*-infected hamster groups compared with a normal group at different time points (21 days and 1, 3, 4, and 5 months postinfection). (B) The mRNA expression level of ANXA1 was evaluated by quantitative real-time RT-PCR. Data were derived from duplicate independent experiments on all five livers in each group and are presented as means ± SD. Statistical significance compared to the normal group, as determined by the Student *t* test: *, $P < 0.05$; ** $P < 0.01$; ***, $P < 0.001$. D, days; M, months; OV, *Opisthorchis viverrini*.

down-modulating leukocyte tissue localization (45). Alternatively, decreased expression of ANXA1 at 1 month might be related to a switching from innate immunity during acute infection (35) to an adaptive response in chronic infection. Therefore, up- or downregulated expression of ANXA1 might occur in differing ways in innate and adaptive immune cells to mediate the resolution of inflammation (35) according to time and endogenous regulators such as IL-1 (39).

More recently, in hamsters infected with *O. viverrini* and treated with *N*-dimethylnitrosamine to induce CCA, enhanced expression of ANXA1 was found in the cytoplasm of inflammatory cells, bile duct epithelial cells, and tumor cells, in proportion to CCA development. Relevantly, ANXA1 levels were higher than in healthy individuals and proved to be a marker for CCA but not for hepatocellular carcinoma (46). The role of ANXA1 in the host response to opisthorchiasis is likely to be important and requires much further study.

In conclusion, this study shows a global impact on protein expression and cytokine/chemokine secretion in PBMCs stimulated with products of live *O. viverrini*. Several proteins were differentially expressed in the PBMCs. Among these, ANXA1 was upregulated in the stimulated human PBMCs, probably via IL-1β stimulation, as well as in inflammatory cells and epithelial bile duct cells of livers in infected hamsters. ANXA1 is an interesting candidate protein for further investigation in relation to its role in pathogenesis of opisthorchiasis. In addition, several acute-phase cytokines/chemokines secreted by PBMCs may play important roles not only in the host response against *O. viverrini* infection but also in pathogenesis of opisthorchiasis.

ACKNOWLEDGMENTS

This work was supported by The Office of the Higher Education Commission, Thailand (Strategic Scholarships for Frontier Research Network for the Ph.D. Program Thai Doctoral degree), the Higher Education Research Promotion and National Research University Project of Thailand, Office of the Higher Education Commission, through the Health Cluster (SHeP-GMS1165), the Khon Kaen University Research Foundation (KKU550401), and the Invitation Research from Faculty of Medicine (I5513).

We thank the Research Assistant (AS53101) from Faculty of Medicine, Khon Kaen University. We thank David Blair for his critical reading and advice on manuscript preparation, and we also thank the Khon Kaen University Publication Clinic, Research and Technology Transfer Affairs, Khon Kaen University, for their assistance.

REFERENCES

1. **IARC.** 2012. *Opisthorchis viverrini* and *Clonorchis sinensis*. IARC Monogr. Eval. Carcinog. Risks Hum. **100B:**341–370.
2. **Sripa B, Bethony JM, Sithithaworn P, Kaewkes S, Mairiang E, Loukas A, Mulvenna J, Laha T, Hotez PJ, Brindley PJ.** 2011. Opisthorchiasis and *Opisthorchis*-associated cholangiocarcinoma in Thailand and Laos. Acta Trop. **120**(Suppl 1):S158–S168. http://dx.doi.org/10.1016/j.actatropica.2010.07.006.
3. **Flavell DJ, Flavell SU.** 1986. *Opisthorchis viverrini*: pathogenesis of infection in immunodeprived hamsters. Parasite. Immunol. **8:**455–466. http://dx.doi.org/10.1111/j.1365-3024.1986.tb00861.x.
4. **Satarug S, Haswell-Elkins MR, Sithithaworn P, Bartsch H, Ohshima H, Tsuda M, Mairiang P, Mairiang E, Yongvanit P, Esumi H, Elkins DB.** 1998. Relationships between the synthesis of *N*-nitrosodimethylamine and immune responses to chronic infection with the carcinogenic parasite, *Opisthorchis viverrini*, in men. Carcinogenesis **19:**485–491. http://dx.doi.org/10.1093/carcin/19.3.485.
5. **Ohshima H, Bartsch H.** 1994. Chronic infections and inflammatory processes as cancer risk factors: possible role of nitric oxide in carcinogen-

esis. Mutat. Res. **305:**253–264. http://dx.doi.org/10.1016/0027-5107(94)90245-3.
6. **Prakobwong S, Pinlaor S, Yongvanit P, Sithithaworn P, Pairojkul C, Hiraku Y.** 2009. Time profiles of the expression of metalloproteinases, tissue inhibitors of metalloproteases, cytokines and collagens in hamsters infected with *Opisthorchis viverrini* with special reference to peribiliary fibrosis and liver injury. Int. J. Parasitol. **39:**825–835. http://dx.doi.org/10.1016/j.ijpara.2008.12.002.
7. **Bhamarapravati N, Thammavit W, Vajrasthira S.** 1978. Liver changes in hamsters infected with a liver fluke of man, *Opisthorchis viverrini*. Am. J. Trop. Med. Hyg. **27:**787–794.
8. **Oberholzer A, Oberholzer C, Moldawer LL.** 2000. Cytokine signaling—regulation of the immune response in normal and critically ill states. Crit. Care. Med. **28:**N3–N12. http://dx.doi.org/10.1097/00003246-200004001-00002.
9. **Finkelman FD, Shea-Donohue T, Goldhill J, Sullivan CA, Morris SC, Madden KB, Gause WC, Urban JF, Jr.** 1997. Cytokine regulation of host defense against parasitic gastrointestinal nematodes: lessons from studies with rodent models. Annu. Rev. Immunol. **15:**505–533. http://dx.doi.org/10.1146/annurev.immunol.15.1.505.
10. **Grencis RK.** 2001. Cytokine regulation of resistance and susceptibility to intestinal nematode infection—from host to parasite. Vet. Parasitol. **100:**45–50. http://dx.doi.org/10.1016/S0304-4017(01)00482-4.
11. **Jittimanee J, Sermswan RW, Puapairoj A, Maleewong W, Wongratanacheewin S.** 2007. Cytokine expression in hamsters experimentally infected with *Opisthorchis viverrini*. Parasite. Immunol. **29:**159–167. http://dx.doi.org/10.1111/j.1365-3024.2006.00929.x.
12. **Sripa B, Mairiang E, Thinkhamrop B, Laha T, Kaewkes S, Sithithaworn P, Tessana S, Loukas A, Brindley PJ, Bethony JM.** 2009. Advanced periductal fibrosis from infection with the carcinogenic human liver fluke *Opisthorchis viverrini* correlates with elevated levels of interleukin-6. Hepatology **50:**1273–1281. http://dx.doi.org/10.1002/hep.23134.
13. **Sripa B, Thinkhamrop B, Mairiang E, Laha T, Kaewkes S, Sithithaworn P, Periago MV, Bhudhisawasdi V, Yonglitthipagon P, Mulvenna J, Brindley PJ, Loukas A, Bethony JM.** 2012. Elevated plasma IL-6 associates with increased risk of advanced fibrosis and cholangiocarcinoma in individuals infected by *Opisthorchis viverrini*. PLoS Negl. Trop. Dis. **6:**e1654. http://dx.doi.org/10.1371/journal.pntd.0001654.
14. **Ninlawan K, O'Hara SP, Splinter PL, Yongvanit P, Kaewkes S, Surapaitoon A, LaRusso NF, Sripa B.** 2010. *Opisthorchis viverrini* excretory/secretory products induce toll-like receptor 4 upregulation and production of interleukin 6 and 8 in cholangiocyte. Parasitol. Int. **59:**616–621. http://dx.doi.org/10.1016/j.parint.2010.09.008.
15. **Khoontawad J, Wongkham C, Hiraku Y, Yongvanit P, Prakobwong S, Boonmars T, Pinlaor P, Pinlaor S.** 2010. Proteomic identification of peroxiredoxin 6 for host defence against *Opisthorchis viverrini* infection. Parasite. Immunol. **32:**314–323. http://dx.doi.org/10.1111/j.1365-3024.2009.01189.x.
16. **Lim LH, Pervaiz S.** 2007. Annexin 1: the new face of an old molecule. FASEB. J. **21:**968–975. http://dx.doi.org/10.1096/fj.06-7464rev.
17. **Khoontawad J, Laothong U, Roytrakul S, Pinlaor P, Mulvenna J, Wongkham C, Yongvanit P, Pairojkul C, Mairiang E, Sithithaworn P, Pinlaor S.** 2012. Proteomic identification of plasma protein tyrosine phosphatase alpha and fibronectin associated with liver fluke, *Opisthorchis viverrini*, infection. PLoS One **7:**e45460. http://dx.doi.org/10.1371/journal.pone.0045460.
18. **Ellerin T, Rubin RH, Weinblatt ME.** 2003. Infections and anti-tumor necrosis factor alpha therapy. Arthritis. Rheum. **48:**3013–3022. http://dx.doi.org/10.1002/art.11301.
19. **Juttner S, Bernhagen J, Metz CN, Rollinghoff M, Bucala R, Gessner A.** 1998. Migration inhibitory factor induces killing of *Leishmania major* by macrophages: dependence on reactive nitrogen intermediates and endogenous TNF-α. J. Immunol. **161:**2383–2390.
20. **Silva JS, Vespa GN, Cardoso MA, Aliberti JC, Cunha FQ.** 1995. Tumor necrosis factor alpha mediates resistance to *Trypanosoma cruzi* infection in mice by inducing nitric oxide production in infected gamma interferon-activated macrophages. Infect. Immun. **63:**4862–4867.
21. **Dinarello CA.** 2009. Immunological and inflammatory functions of the interleukin-1 family. Annu. Rev. Immunol. **27:**519–550. http://dx.doi.org/10.1146/annurev.immunol.021908.132612.
22. **Pinlaor S, Tada-Oikawa S, Hiraku Y, Pinlaor P, Ma N, Sithithaworn P, Kawanishi S.** 2005. *Opisthorchis viverrini* antigen induces the expression of Toll-like receptor 2 in macrophage RAW cell line. Int. J. Parasitol. **35:**591–596. http://dx.doi.org/10.1016/j.ijpara.2005.02.003.
23. **Pinlaor S, Hiraku Y, Ma N, Yongvanit P, Semba R, Oikawa S, Murata M, Sripa B, Sithithaworn P, Kawanishi S.** 2004. Mechanism of NO-mediated oxidative and nitrative DNA damage in hamsters infected with *Opisthorchis viverrini*: a model of inflammation-mediated carcinogenesis. Nitric Oxide **11:**175–183. http://dx.doi.org/10.1016/j.niox.2004.08.004.
24. **Boockvar KS, Granger DL, Poston RM, Maybodi M, Washington MK, Hibbs JB, Jr, Kurlander RL.** 1994. Nitric oxide produced during murine listeriosis is protective. Infect. Immun. **62:**1089–1100.
25. **James SL, Hibbs JB, Jr.** 1990. The role of nitrogen oxides as effector molecules of parasite killing. Parasitol. Today **6:**303–305. http://dx.doi.org/10.1016/0169-4758(90)90261-2.
26. **Liew FY, Millott S, Parkinson C, Palmer RM, Moncada S.** 1990. Macrophage killing of *Leishmania* parasite in vivo is mediated by nitric oxide from L-arginine. J. Immunol. **144:**4794–4797.
27. **Hashimoto M, Shingu M, Ezaki I, Nobunaga M, Minamihara M, Kato K, Sumioki H.** 1994. Production of soluble ICAM-1 from human endothelial cells induced by IL-1 β and TNF-α. Inflammation **18:**163–173. http://dx.doi.org/10.1007/BF01534557.
28. **Witkowska AM, Borawska MH.** 2004. Soluble intercellular adhesion molecule-1 (sICAM-1): an overview. Eur. Cytokine. Netw. **15:**91–98. http://www.jle.com/en/revues/bio_rech/ecn/e-docs/00/04/04/20/article.phtml.
29. **Deshmane SL, Kremlev S, Amini S, Sawaya BE.** 2009. Monocyte chemoattractant protein-1 (MCP-1): an overview. J. Interferon Cytokine Res. **29:**313–326. http://dx.doi.org/10.1089/jir.2008.0027.
30. **Dufour JH, Dziejman M, Liu MT, Leung JH, Lane TE, Luster AD.** 2002. IFN-γ-inducible protein 10 (IP-10; CXCL10)-deficient mice reveal a role for IP-10 in effector T cell generation and trafficking. J. Immunol. **168:**3195–3204. http://www.jimmunol.org/content/168/7/3195.long.
31. **Keepers TR, Gross LK, Obrig TG.** 2007. Monocyte chemoattractant protein 1, macrophage inflammatory protein 1 alpha, and RANTES recruit macrophages to the kidney in a mouse model of hemolytic-uremic syndrome. Infect. Immun. **75:**1229–1236. http://dx.doi.org/10.1128/IAI.01663-06.
32. **Marder SR, Chenoweth DE, Goldstein IM, Perez HD.** 1985. Chemotactic responses of human peripheral blood monocytes to the complement-derived peptides C5a and C5a des Arg. J. Immunol. **134:**3325–3331.
33. **Kamanaka M, Yu P, Yasui T, Yoshida K, Kawabe T, Horii T, Kishimoto T, Kikutani H.** 1996. Protective role of CD40 in *Leishmania major* infection at two distinct phases of cell-mediated immunity. Immunity **4:**275–281. http://dx.doi.org/10.1016/S1074-7613(00)80435-5.
34. **Yongvanit P, Thanan R, Pinlaor S, Sithithaworn P, Loilome W, Namwat N, Techasen A, Dechakhamphu S.** 2012. Increased expression of TLR-2, COX-2, and SOD-2 genes in the peripheral blood leukocytes of opisthorchiasis patients induced by *Opisthorchis viverrini* antigen. Parasitol. Res. **110:**1969–1977. http://dx.doi.org/10.1007/s00436-011-2725-5.
35. **Perretti M, D'Acquisto F.** 2009. Annexin A1 and glucocorticoids as effectors of the resolution of inflammation. Nat. Rev. Immunol. **9:**62–70. http://dx.doi.org/10.1038/nri2470.
36. **Solito E, Christian HC, Festa M, Mulla A, Tierney T, Flower RJ, Buckingham JC.** 2006. Post-translational modification plays an essential role in the translocation of annexin A1 from the cytoplasm to the cell surface. FASEB. J. **20:**1498–1500. http://dx.doi.org/10.1096/fj.05-5319fje.
37. **Bizzarro V, Petrella A, Parente L.** 2012. Annexin A1: novel roles in skeletal muscle biology. J. Cell. Physiol. **227:**3007–3015. http://dx.doi.org/10.1002/jcp.24032.
38. **Mimura KK, Tedesco RC, Calabrese KS, Gil CD, Oliani SM.** 2012. The involvement of anti-inflammatory protein, annexin A1, in ocular toxoplasmosis. Mol. Vis. **18:**1583–1593. http://www.ncbi.nlm.nih.gov/pmc/articles/PMC3382303/.
39. **Morand EF, Hall P, Hutchinson P, Yang YH.** 2006. Regulation of annexin I in rheumatoid synovial cells by glucocorticoids and interleukin-1. Mediators Inflamm. **2006:**73835. http://dx.doi.org/10.1155/MI/2006/73835.
40. **Leoni G, Alam A, Neumann PA, Lambeth JD, Cheng G, McCoy J, Hilgarth RS, Kundu K, Murthy N, Kusters D, Reutelingsperger C, Perretti M, Parkos CA, Neish AS, Nusrat A.** 2013. Annexin A1, formyl peptide receptor, and NOX1 orchestrate epithelial repair. J. Clin. Invest. **123:**443–454. http://dx.doi.org/10.1172/JCI65831.
41. **Seth D, Leo MA, McGuinness PH, Lieber CS, Brennan Y, Williams R, Wang XM, McCaughan GW, Gorrell MD, Haber PS.** 2003. Gene expression profiling of alcoholic liver disease in the baboon (*Papio hama-*

dryas) and human liver. Am. J. Pathol. **163:**2303–2317. http://dx.doi.org/10.1016/S0002-9440(10)63587-0.
42. **de Coupade C, Gillet R, Bennoun M, Briand P, Russo-Marie F, Solito E.** 2000. Annexin 1 expression and phosphorylation are upregulated during liver regeneration and transformation in antithrombin III SV40 T large antigen transgenic mice. Hepatology **31:**371–380. http://dx.doi.org/10.1002/hep.510310217.
43. **Sripa B, Kaewkes S.** 2000. Localisation of parasite antigens and inflammatory responses in experimental opisthorchiasis. Int. J. Parasitol. **30:**735–740. http://dx.doi.org/10.1016/S0020-7519(00)00054-0.
44. **Pinlaor S, Sripa B, Sithithaworn P, Yongvanit P.** 2004. Hepatobiliary changes, antibody response, and alteration of liver enzymes in hamsters re-infected with *Opisthorchis viverrini*. Exp. Parasitol. **108:**32–39. http://dx.doi.org/10.1016/j.exppara.2004.07.007.
45. **Perretti M.** 1998. Lipocortin 1 and chemokine modulation of granulocyte and monocyte accumulation in experimental inflammation. Gen. Pharmacol. **31:**545–552. http://dx.doi.org/10.1016/S0306-3623(98)00039-1.
46. **Hongsrichan N, Rucksaken R, Chamgramol Y, Pinlaor P, Techasen A, Yongvanit P, Khuntikeo N, Pairojkul C, Pinlaor S.** 2013. Annexin A1: a new immunohistological marker of cholangiocarcinoma. World J. Gastroenterol. **19:**2456–2465. http://dx.doi.org/10.3748/wjg.v19.i16.2456.